An Advanced Battery Charging System using Bipolar Pulse Strategy for Lithium-ion Battery Durability Enhancement

Yujie Ding[1,2], Haimeng Wu[2], Mousa Marzband[2]
Bing Ji[3] and Jianfeng Zhao[1]

[1] Southeast University, Nanjing, Jiangsu, China
[2] Northumbria University, Newcastle. NE1 8ST, UK
[3] School of Engineering, University of Leicester, UK
haimeng.wu@northumbria.ac.uk

Abstract. With the increasing deployment of energy storage devices in electric vehicles and distributed renewable power network, the extensive research on battery charging systems has shown a growing significance. This paper focuses on developing a new charging method which aims at extending the lifespan of lithium-ion battery by using bipolar current pulses. A battery charging system employing a phase-shift controlled dual active bridge and battery elements has been studied and its small-signal average model is established to investigate the dynamic control of the proposed bipolar pulse charging approach. Furthermore, the influence of the negative pulse on eliminating the polarization effect and inhibiting the ageing of the lithium-ion battery has been analyzed in detail. Finally, an advanced four-stage battery charging strategy is proposed to achieve the suppression of the ageing effect and potentially extend the battery life, which also shows a 7.58% reduction of the total charging time compared with the traditional charging method.

Keywords: Battery Charger, Power Converters, Battery Charging Approach, Bipolar Pulse, Battery Lifespan.

1 Introduction

Electric-driven transportation is to be in extensive use due to its high efficiency and the potential benefits in terms of reduced carbon emissions [1, 2]. Lithium-ion batteries are widely used in electric vehicles (EVs) as critical energy storage devices due to their high energy density, low self-discharge rate, and good repeated charge and discharge characteristics [3]. At present, a large quantity of research is devoted to improving the charging rate and efficiency of the charging system from the perspective of the topologies and control strategies of the power converters as well as the modelling and characterization of the battery [4-9]. However, in addition to charging rate and efficiency, it is essential to investigate the advanced charging approach to extend the lifespan of the battery because this significantly affects the battery's service life for EVs. In other words, the extension of the durability of the battery can effectively increase the actual battery capacity after hundreds of charge and discharge cycles, and reduces the system maintenance cost.

In terms of the battery charging strategies, the constant current constant voltage (CC-CV) charging is a classical method that has been widely used in the industry because of its simplicity and ease of control. Many other charging approaches have been presented in recent years. A multi-objective optimal charging approach is developed to decrease the charging time and relieve the battery degradation [10], which is mainly focused on the trade-off between charging duration and battery aging process. A variable frequency and variable duty cycle pulse charging method based on the AC impedance characteristics of the battery has been proposed to maximize the energy conversion efficiency [11], but this method shows the limits on the high cost of the devices generating high-frequency current pulses as well as the challenges of obtaining different battery frequency characteristics. To measure the open-circuit voltage of batteries in a short time, a one-cycle bipolar-current pulse method is proposed in [12] However, this approach is mainly developed for the rapid estimation of state-of-charge (SOC) of battery which is not designed for excessive charging process. In [13], a constant-temperature constant-voltage charging technique is proposed to help reduce battery ageing caused by overheating, whereas the damage to the battery caused by the large charging current in the low state of charge (SOC) region has been neglected in the study. Moreover, to cope with the issue of polarization voltage in batteries, a constant polarization voltage charging method is proposed in [14] and the relationship between polarization voltage and SOC has been discussed. Also, this method reveals that the polarization voltage is an approximate external manifestation of the battery's chemical reaction rate and charge acceptance.

In this paper, a novel four-stage charging strategy with bipolar current pulses is proposed to prolong the lifespan and to increase the charging capability of the lithium-ion battery. A battery charging system utilizing a dual active bridge (DAB) DC-DC converter has been developed and analyzed in detail, and the obtained small-signal model is used to study the system dynamic control. The effect of the negative pulse on reducing the polarization effect is examined using an equivalent battery model, and the proposed charging approach cannot only reduce 7.58 percent of the charging time compared to the traditional CC-CV charging, but also be beneficial to prolong the battery life.

2 Theoretical Principle

2.1 Battery model

From the perspective of the external characteristics of the battery, a universal equivalent model of the lithium-ion battery is composed of an open-circuit voltage (OCV) source, an ohmic resistance, and a resistance-capacitance network that reflects the polarization phenomenon [14], as is shown in Fig. 1. A first-order Thevenin equivalent model can be adopted for the analysis of the negative pulse on eliminating polarization effect since the attenuation time constant of an RC pair is substantially larger than the possible negative pulse adopted. If a higher precision is required, a second-order Thevenin equivalent model can be used in the modelling of the battery pack.

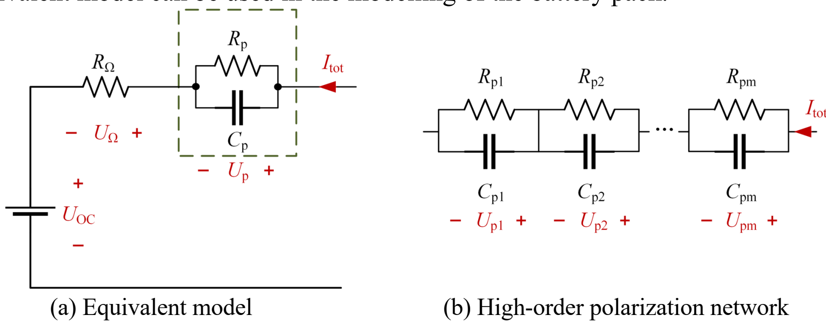

Fig. 1. A universal Thevenin equivalent model of battery

The influence of the charge and discharge current on the polarization effect is analyzed as follows. The battery model can be expressed as

$$\begin{cases} C_p \dfrac{dU_p}{dt} + \dfrac{U_p}{R_p} = i_{tot} \\ U_{tml} - U_p - U_\Omega = U_{OC} \\ p_{loss} = i_{tot}^2 R_\Omega + \dfrac{U_p^2}{R_p} \end{cases} \tag{1}$$

where U_{tml} is the terminal voltage of the battery, U_{OC} is the battery internal potential OCV, U_Ω is the ohmic internal potential which is proportional to the charge and discharge current, and U_p represents the polarization potential that has a gradual decay process after the removal of charge and discharge current; R_Ω, R_p, and C_p are the equivalent parameters of the battery; i_{tot} refers to the total charge or discharge current, and p_{loss} refers to the total power loss on the internal resistance of the battery.

By solving (1), the time domain expression of the polarization voltage is obtained as

$$U_p(t) = e^{-\frac{1}{R_p C_p}(t-t_0)} U_p(t_0) + \frac{1}{C_p} e^{-\frac{1}{R_p C_p}t} \int_{t_0}^{t} e^{\frac{1}{R_p C_p}\tau} i(\tau) d\tau \tag{2}$$

In practice, a continuous charging or discharging process can be regarded as a series of CC segments applied to the battery in every short period of time, thereby the difference model can be obtained by discretizing from (2) as

$$\begin{cases} U_p[k+1] = e^{-\frac{1}{R_p C_p}T_s} U_p[k] + R_p(1 - e^{-\frac{1}{R_p C_p}T_s}) i_{tot}[k] \\ p_{loss}[k] = \dfrac{1}{R_p} U_p^2[k] + R_\Omega i_{tot}^2[k] \end{cases} \tag{3}$$

where T_s is the incremental time during iterations.

Due to the negative current pulse serves as a critical component in the bipolar pulse charging strategy, its effect on the elimination of polarization voltage after a positive pulse is explained as follows. The loss of the RC pair is proportional to the square of the current flowing through the polarization resistance, that is, proportional to the square of the polarization voltage. As a result, in order to reduce polarization, the optimal magnitude of the negative pulse should be reduced to 0 as quickly as possible, which is shown in the following

$$i_{\text{tot}}\left[k\right]=-\frac{e^{-\frac{1}{R_{\text{p}}C_{\text{p}}}T_{\text{s}}}U_{\text{p}}\left[k\right]}{R_{\text{p}}(1-e^{-\frac{1}{R_{\text{p}}C_{\text{p}}}T_{\text{s}}})} \tag{4}$$

This can be obtained by setting $U_{\text{p}}\left[k+1\right]$ equals zero in (3). Besides, the result of (4) should be cut off within the acceptable discharge rate of the battery.

2.2 System-level Modelling

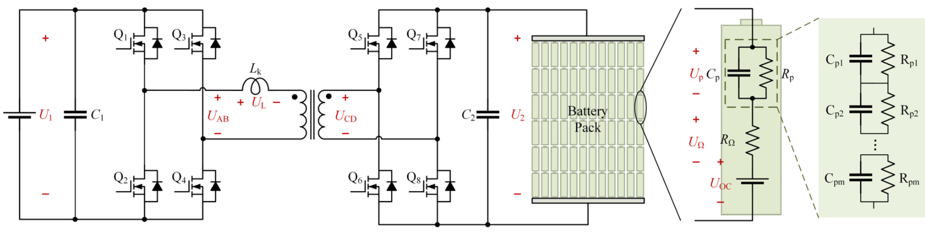

Fig. 2. Schematic of the charging system

The dual active full-bridge DC-DC converter with a battery load is presented in Fig. 2. This topology has the following advantages that is regarded as one of the best solutions for EV's battery chargers. Firstly, in comparison to non-isolated DC-DC converters, a high-frequency transformer in the topology creates electrical isolation between the input and output terminals, which improves the converter's safety and reliability for electrified transportation[15, 16]. Second, this topology is capable of transmitting high power for fast charging technique. In contrast, the power capacity of the Forward [17], the Flyback [15], and the Push-pull DC-DC converter [18] is limited due to the high switch voltage stress. Thirdly, the DAB DC-DC converter can achieve rapid bidirectional power transmission and ease to realize soft-switching under phase shift control.

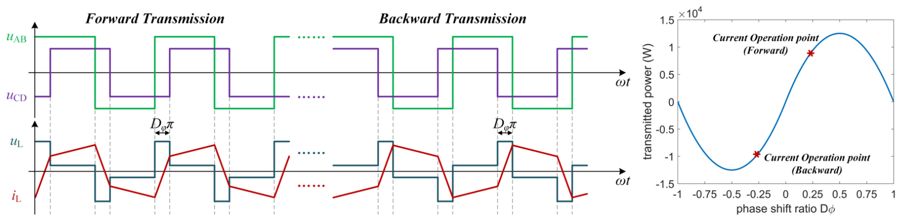

Fig. 3. Key operation waveforms of the DAB DC-DC converter

In a typical phase-shift controlled DAB DC-DC converter, the two power switches on the same side of each bridge arm turn on and off complementary with a phase difference of 180°, and the diagonal switches of each full bridge are normally turned on and off at the same time as is shown in Fig. 3. There is a voltage applied to the leakage inductor which is generated by the operation of the active switches at the primary and secondary sides. The transmitted power and power flow direction under steady-state can be controlled by the values of phase shift angle and the leading/lagging relationship of the voltages across the leakage inductor respectively. The power transmission can be determined by using the equation as follows:

$$P=U_1\frac{1}{T_s}\int_0^{T_s} i_L(t)dt=\frac{nU_1U_2}{2fL_k}D_\varphi(1-D_\varphi) \tag{5}$$

where U_1 is the input voltage, U_2 is the output voltage, n is the winding ratio of the transformer, f is the switching frequency, L_k is the total leakage inductance, and D_φ is the phase shift ratio, which is the phase-shift angle divided by π.

From (5) it can be seen that the direction of power transmission can be quickly switched by changing the polarity of the phase shift angle, , i.e., when $D_\varphi > 0$ which means the forward power transmission from primary to secondary side, vice versa, when $D_\varphi < 0$, it indicates the reverse power transmission.

The small-signal average model of the system is obtained by applying small disturbances to the steady-state model. Considering that the input and output currents are both alternative currents due to the leakage inductance of the circuit, the periodic average value of the power side current and the battery side current is denoted as I_{1avg} and I_{2avg}. And the expressions of the currents can be obtained as follows according to (5),

$$I_{1avg}=\frac{nU_2}{2fL_k}D_\varphi(1-D_\varphi) \tag{6}$$

$$I_{2avg}=\frac{nU_1}{2fL_k}D_\varphi(1-D_\varphi) \tag{7}$$

By applying the small disturbances and utilizing the first-order Taylor formula, the mathematic formulation of the small-signal average model of the DAB DC-DC converter can be obtained as follows:

$$\hat{i}_{2avg}=\frac{\partial I_{2avg}}{\partial D_\varphi}\hat{d}_\varphi+\frac{\partial I_{2avg}}{\partial U_1}\hat{u}_1=g_{2d}\hat{d}_\varphi+g_{2u_1}\hat{u}_1 \tag{8}$$

$$\hat{i}_{1avg}=\frac{\partial I_{1avg}}{\partial D_\varphi}\hat{d}_\varphi+\frac{\partial I_{1avg}}{\partial U_2}\hat{u}_2=g_{1d}\hat{d}_\varphi+g_{1u_2}\hat{u}_2 \tag{9}$$

where $\hat{u}_1$, $\hat{u}_2$, $\hat{i}_{1avg}$, $\hat{i}_{2avg}$, and $\hat{d}_\varphi$ refers to the small disturbance of the supply side voltage, the battery side voltage, the periodic average input current, the periodic average output current, and the phase shift ratio. In addition, $g_{2\mathrm{d}}=\frac{nU_1}{2fL_\mathrm{k}}(1-2D)$, $g_{1\mathrm{d}}=\frac{nU_2}{2fL_\mathrm{k}}(1-2D)$, and $g_{2\mathrm{u}_1}=g_{1\mathrm{u}_2}=\frac{n}{2fL_\mathrm{k}}D(1-D)$.

Thereby following the small-signal average model of the DAB DC-DC converter with lithium-ion battery pack, the dynamic model of the system can be drawn as Fig. 4.

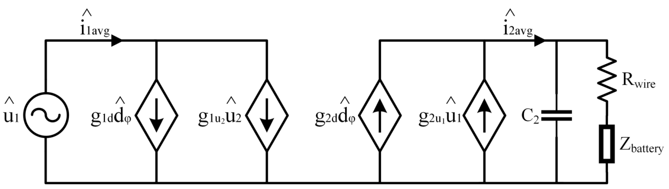

Fig. 4. The small-signal average model of the DAB DC-DC converter

Hence, the output transfer function is shown as (10), which can be used for controller design.

$$\widehat{u_2}=\frac{1+R_\mathrm{eq}C_\mathrm{eq}s}{C_2R_\mathrm{eq}C_\mathrm{eq}s^2+(C_2+C_\mathrm{eq})s}\left(g_{2\mathrm{d}}\hat{d}_\varphi+g_{2\mathrm{u}_1}\widehat{u_1}\right) \tag{10}$$

where R_eq equals $R_{wire}+\mathrm{Re}[Z_{battery}]$, C_eq equals $\mathrm{Im}[Z_{battery}]/s$, and C_2 is the capacitor at the battery side.

2.3 Charging Strategy

It was found that pulsed current can reduce concentration polarization and interface resistance [19], which helps improve the discharge capacity and cycle life of lithium-ion batteries. In addition, by adding negative pulse, the bipolar pulse charging method is capable of uniformly depositing lithium, limiting the growth of lithium dendrites [20].

Charging with mixed positive and negative pulses has a significant effect on inhibiting battery ageing and weakening the polarization effect. The three-stage charging method is widely used in the industry, which is composed of the pre-charging stage, the constant current stage, and the constant voltage stage (PC-CC-CV). Based on this, a novel four-stage charging method is proposed with a tradeoff among the total charging time, charging efficiency, and anti-ageing, which consists of a pre-charging stage, a constant current stage, a bipolar pulse stage, and a constant voltage stage (PC-CC-BP-CV). The flowchart of the proposed four stage PC-CC-BP-CV charging strategy is shown in Fig. 5. The bipolar pulse charging stage is employed in the middle and late periods of the charging process in order to minimize the extra loss produced by the negative pulse in the ohmic resistance. Also, it should be considered that the polarization effect is more dramatic in the high SOC area.

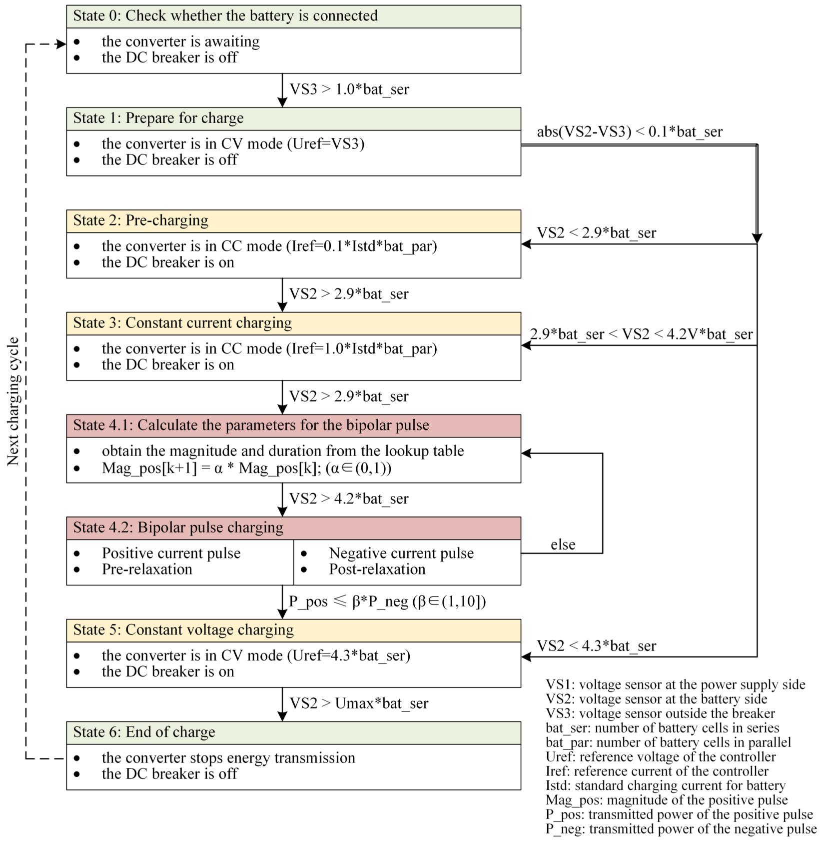

Fig. 5. Flowchart of the proposed PC-CC-BP-CV charging strategy

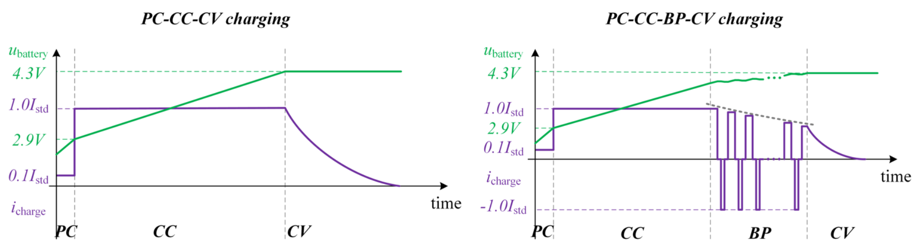

Fig. 6. Flowchart of the proposed PC-CC-BP-CV charging strategy

The whole charging schematic is presented in Fig. 6. The pre-charging stage uses a small charging current (usually 0.1 of the recommended maximum charging current) to smoothly raise the battery internal voltage OCV because of the large gradient to the SOC at this stage; Compared with the classical three-stage charging method, in the proposed charging strategy, bipolar current pulses replace most of the charging time in the CV stage, which is to attenuate the polarization voltage, to inhibit the precipitation and adhesion of lithium crystals on the surface of the battery plate, as well as uniform the distribution of the electrolyte. The magnitude of the positive current pulse is designed to decay proportionally to the cycle time of State 4.1 and State 4.2 considering the reduced current acceptance of the battery at the end of the charging process; The final short-time CV stage is also needed due to preventing voltage overshoot.

3 Simulation evaluation

3.1 Dynamic control of the Power converter

To achieve a fast transient state control of the DAB DC-DC converter, a discrete incremental PI controller is used. A Bode diagram of the system is constructed according to the small-signal average model proposed earlier, as illustrated in Fig. 7. By increasing 30 dB of the static gain and accelerating the decrease of the magnitude response at the mid frequency band, the controller contributes to the elimination of steady-state error and the enhancement of dynamic response.

Fig. 8 shows the dynamic performance of the converter using the designed controller, which can demonstrate that the system can quickly switch the direction of energy transmission and stabilize within 500 us. Also, the waveforms of the transient voltage and current are given to show how they perform at the fast transients.

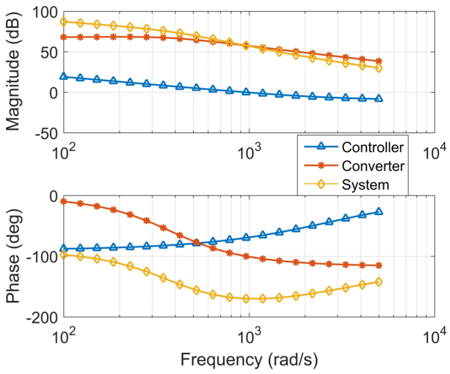

Fig. 7. Bode diagram of the system

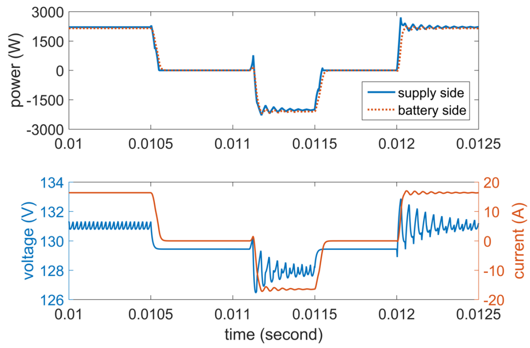

Fig. 8. Transient waveforms during the conversion of the power flow

3.2 Analysis of depolarization effects

The RC parallel network of the battery is numerically simulated in Matlab/Simulink in order to determine the amplitude and duration of the optimal negative pulse current. The loss and the optimal negative pulse current amplitude are calculated according to (3) and (4), and the results are shown below. Fig. 9 (a) shows the decay curve of the polarization voltage under negative pulses with different amplitudes, which verifies the significant effect of the negative pulse on reducing the polarization effect. Fig. 9 (b) illustrates that a large pulse amplitude is beneficial to eliminate the polarization effect within a given time, and before the polarization voltage reaches zero, the maximum negative pulse current allowed is inclined to be selected. Fig. 9 (c) shows that the negative pulse current reduces the loss of the internal polarization resistance during the whole process. Compared with the loss without a negative pulse, the loss on the RC pair is reduced 28.28%, 49.11%, 62.53% and 70.45% in the case of 1 CC, 2 CC, 3 CC, and 4 CC respectively. However, given the battery's durability and the loss of negative pulse current due to ohmic resistance, setting the amplitude and length of the practical negative pulse as large as feasible is not recommended.

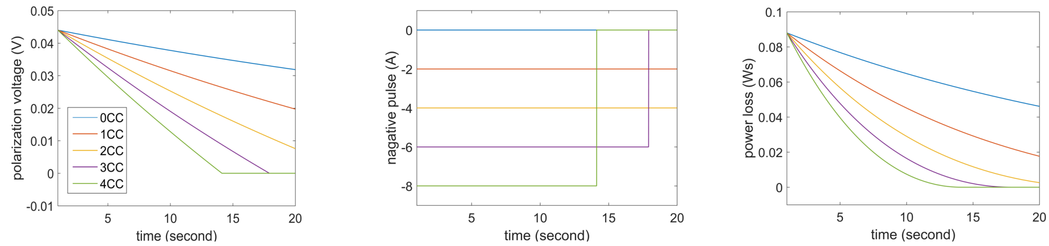

(a) attenuation of the polarization voltage (b) magnitude of the negative pulse (c) power loss on the RC pair

Fig. 9. Effect of negative pulse current on the elimination of polarization voltage

3.3 Bipolar pulse charging

Fig. 10 shows a full diagram of the battery charging system with control, including a DAB DC-DC converter, a charging management system, and a second-order battery pack model. The parameters of the converter and battery pack model are shown in Table 1 and Table 2, respectively. The second-order Thevenin equivalent battery model is used to provide precise polarization effect simulation, and the parameters of the components in the battery model are obtained using the hybrid pulse power characterization (HPPC) test. To run the simulation efficiently, the battery model is built to include a simulation acceleration capability that works in tandem with the power conversion stage.

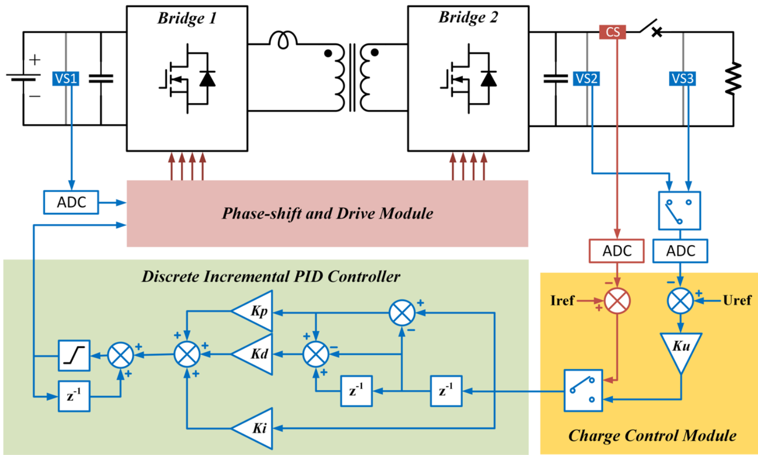

Fig. 10. Diagram of the battery charging system with control

Table 1. Parameters of the DAB DC-DC converter

Maximum power transmission	12.5 kW
Switch frequency	20 kHz
Total leakage inductance	20 μH
Supply side voltage	200 V
Battery side voltage	150 V
DC Capacitor	100 μF

Table 2. Parameters of the NCR18650B battery pack model

Cell nominal voltage	3.6 V
Rated capacity	3350 mAh
Standard charging current	1625 mA
Number of batteries in series	35
Number of batteries in parallel	35
Initial SOC	20 %
Romic	0.076 Ohm
Rp1	0.022 Ohm
Rp2	0.0151 Ohm
Cp1	2674.5 Farad
Cp2	95695.4 Farad

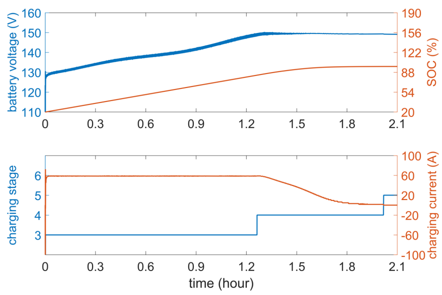

(a) PC-CC-CV charging

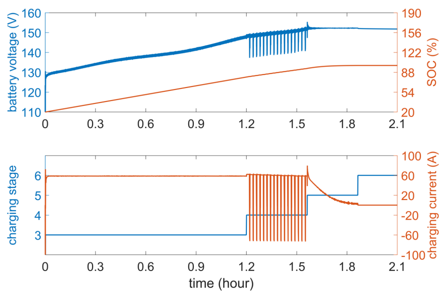

(b) PC-CC-BP-CV charging

Fig. 11. Waveforms under different charging methods

The PC-CC-CV charging and PC-CC-BP-CV charging approaches are implemented in the developed simulation model, and the key waveforms of which are shown in Fig. 11 (a) and Fig. 11 (b) respectively. Table 3 shows the converted charging time and energy loss. Compared with the PC-CC-CV charging method, the charging time of the proposed method is reduced by 7.58%. Because the bipolar pulse current flows through the battery internal resistance during the positive and negative pulses, it causes a 3.37%

increase of the total energy loss. However, because the bipolar pulse can inhibit the precipitation of lithium crystals and prolong the battery life, the slight increase in loss is worthwhile. In summary, the simulation results verify the effectiveness of the control strategy and demonstrate a good performance of the proposed charging strategy.

Table 3. Charging time and energy loss after conversion

Charging method	PC-CC-CV	PC-CC-BP-CV
Charging time (h)	2.019	1.866
Battery loss (kWh)	0.557	0.602
Converter loss (kWh)	1.044	1.053

4 Conclusion

This research presents a full charging scheme utilizing bipolar pulses aimed at prolonging the lifespan of lithium-ion batteries. A small-signal average model of the DAB DC-DC converter with battery load is developed to investigate the dynamic control of bipolar charging pulses, which indicates that it can generate bipolar current pulses effectively without the need for additional circuits. The study of the negative pulse effect demonstrates the advantages of bipolar charging in terms of reducing the polarization effect and anti-aging. Finally, a novel PC-CC-BP-CV charging strategy is proposed to suppress the ageing of the battery, which also saves charging time by 7.58% compared with the typical CC-CV charging approach. This method can be directly deployed in EV chargers that employ a DAB structure without modifying the hardware or adding additional sensors.

Acknowledgment

The authors would like to thank Department of Mathematics, Physics and Electrical Engineering, Northumbria University, for the full support and research funding.

References

1 Ronald, J.: ‘Electric Vehicles (EV)’: ‘Electric and Hybrid-Electric Vehicles’ (SAE, 2002), pp. 1-1
2 Naseri, F., Farjah, E., and Ghanbari, T.: ‘An Efficient Regenerative Braking System Based on Battery/Supercapacitor for Electric, Hybrid, and Plug-In Hybrid Electric Vehicles With BLDC Motor’, Ieee T Veh Technol, 2017, 66, (5), pp. 3724-3738
3 Jiang, J., Zhang, C., Wen, J., Zhang, W., and Sharkh, S.M.: ‘An Optimal Charging Method for Li-Ion Batteries Using a Fuzzy-Control Approach Based on Polarization Properties’, Ieee T Veh Technol, 2013, 62, (7), pp. 3000-3009
4 Vu, V., Tran, D., and Choi, W.: ‘Implementation of the Constant Current and Constant Voltage Charge of Inductive Power Transfer Systems With the Double-Sided LCC

Compensation Topology for Electric Vehicle Battery Charge Applications', IEEE Transactions on Power Electronics, 2018, 33, (9), pp. 7398-7410
5 Wang, Y., Li, Y., Jiang, L., Huang, Y., and Cao, Y.: 'PSO-based optimization for constant-current charging pattern for li-ion battery', Chinese Journal of Electrical Engineering, 2019, 5, (2), pp. 72-78
6 Parvini, Y., Vahidi, A., and Fayazi, S.A.: 'Heuristic Versus Optimal Charging of Supercapacitors, Lithium-Ion, and Lead-Acid Batteries: An Efficiency Point of View', IEEE Transactions on Control Systems Technology, 2018, 26, (1), pp. 167-180
7 Vangen, K., Melaa, T., Bergsmark, S., and Nilsen, R.: 'Efficient high-frequency soft-switched power converter with signal processor control', in Editor (Ed.)^(Eds.): 'Book Efficient high-frequency soft-switched power converter with signal processor control' (1991, edn.), pp. 631-639
8 Zhan, H., Wu, H., Muhammad, M., Lambert, S., and Pickert, V.: 'Combining electric vehicle battery charging and battery cell equalisation in one circuit', IET Electrical Systems in Transportation, n/a, (n/a)
9 Wu, H., Pickert, V., Lambert, S., Allanf, P., Deng, X., and Zhan, H.: 'A ripple reduction method for a two stages battery charger with multi-winding transformer using notch filter', in Editor (Ed.)^(Eds.): 'Book A ripple reduction method for a two stages battery charger with multi-winding transformer using notch filter' (2017, edn.), pp. 1,101-101,106
10 Gao, Y., Zhang, X., Guo, B., Zhu, C., Wiedemann, J., Wang, L., and Cao, J.: 'Health-Aware Multiobjective Optimal Charging Strategy With Coupled Electrochemical-Thermal-Aging Model for Lithium-Ion Battery', IEEE Transactions on Industrial Informatics, 2020, 16, (5), pp. 3417-3429
11 Amanor-Boadu, J.M., Guiseppi-Elie, A., and Sánchez-Sinencio, E.: 'Search for Optimal Pulse Charging Parameters for Li-Ion Polymer Batteries Using Taguchi Orthogonal Arrays', Ieee T Ind Electron, 2018, 65, (11), pp. 8982-8992
12 Yao, Q., Lu, D.D.C., and Lei, G.: 'Rapid Open-Circuit Voltage Measurement Method for Lithium-Ion Batteries Using One-Cycle Bipolar-Current Pulse', IEEE Journal of Emerging and Selected Topics in Industrial Electronics, 2021, 2, (2), pp. 132-141
13 Wang, S., and Liu, Y.: 'A PSO-Based Fuzzy-Controlled Searching for the Optimal Charge Pattern of Li-Ion Batteries', Ieee T Ind Electron, 2015, 62, (5), pp. 2983-2993
14 Jiang, J., Liu, Q., Zhang, C., and Zhang, W.: 'Evaluation of Acceptable Charging Current of Power Li-Ion Batteries Based on Polarization Characteristics', Ieee T Ind Electron, 2014, 61, (12), pp. 6844-6851
15 Caricchi, F., Crescimbini, F., Capponi, F.G., and Solero, L.: 'Study of bi-directional buck-boost converter topologies for application in electrical vehicle motor drives', in Editor (Ed.)^(Eds.): 'Book Study of bi-directional buck-boost converter topologies for application in electrical vehicle motor drives' (1998, edn.), pp. 287-293 vol.281
16 Sable, D.M., Lee, F.C., and Cho, B.H.: 'A zero-voltage-switching bidirectional battery charger/discharger for the NASA EOS satellite', in Editor (Ed.)^(Eds.): 'Book A zero-voltage-switching bidirectional battery charger/discharger for the NASA EOS satellite' (1992, edn.), pp. 614-621
17 Do, H.: 'Nonisolated Bidirectional Zero-Voltage-Switching DC–DC Converter', IEEE Transactions on Power Electronics, 2011, 26, (9), pp. 2563-2569
18 Chung, H.S.H., Cheung, W.L., and Tang, K.S.: 'A ZCS bidirectional flyback DC/DC converter', Ieee Transactions on Power Electronics, 2004, 19, (6), pp. 1426-1434
19 'IEEE Guide for Selecting, Charging, Testing, and Evaluating Lead-Acid Batteries Used in Stand-Alone Photovoltaic (PV) Systems', IEEE P1361/D5, February 2014, 2014, pp. 1-36
20 Zhu, S.Q., Hu, C., Xu, Y., Jin, Y., and Shui, J.L.: 'Performance improvement of lithium -ion battery by pulse current', J. Energy Chem., 2020, 46, pp. 208-214